CHAPTER 235

MUD TRANSPORT AND MUDDY BOTTOM DEFORMATION BY WAVES

Daoxian SHEN*, Masahiko ISOBE† and Akira WATANABE†

ABSTRACT

The present study focuses on numerical simulation of wave height decay and muddy bottom deformation under wave action. Experiments have been performed to determine the vertical distribution of the water content ratio of mud. Using the experimental results, a simulation model has been set up to estimate change in the water content ratio in the mud bed. Also, a simple one-dimensional numerical model has been developed to predict the muddy bottom deformation under waves as well as the wave height decay. Wave flume experiments have been carried out and the changes in the bottom topography and wave height have been compared with the calculations.

KEYWORDS: Change in water content ratio, Wave height decay, Mud transport, Muddy bottom deformation.

1 Introduction

Along muddy coasts fine grained, cohesive sediment is consistently present in the nearshore waters and around the shoreline. These muddy bed sediments may have a significant effect on the hydrodynamic processes. Prediction of mud transport and resultant bathymetric change due to waves are essential in order to take effective countermeasures against erosion and siltation and to plan rational new works in coastal regions. Although many studies on mud transport under waves and on wave dissipation due to mud motion have been conducted (Gade, 1958; Dalrymple and Liu, 1978; Mei and Liu, 1987; Shibayama, 1993), only few attempts have been reported so far on the prediction of topography change on soft mud beaches.

The establishment of topographical change models for muddy beaches seems to be difficult for three reasons. First, the transport of fine-grained cohesive sediment is quite different from that of coarse-grained sediment. The cohesiveness

*Engineer, Coastal Engineering Consultants Co., Ltd., Tamura Bldg. 3F, Hongo 5-23-13, Bunkyo-ku, Tokyo, 113 Japan

†Professor, Department of Civil Engineering, University of Tokyo, Hongo 7-3-1, Bunkyo-ku, Tokyo, 113 Japan

of soft mud makes its motion under the action of waves and currents more complicated than that of non-cohesive sediment. Second, the vertical structure of the concentration depends on both wave conditions and mud properties. Third, it is difficult to formulate a relationship for the local transport rate under the waves. It may be stated that our knowledge of mud transport processes has not yet reached a level where we can deal with these problems effectively.

On the other hand, the interaction between propagating ocean waves and a stable seabed or consolidated soil has received an extensive attention in the field of offshore and foundation engineering (Yamamoto, 1978; Zen and Yamazaki, 1991). However, their interest is either in the wave-induced liquefaction in a porous seabed or on the problem of unfavorable pore pressure, which could make the seabed or an offshore structure unstable.

The present study focuses on the numerical simulation of wave height decay and muddy bottom deformation under wave action. First, the vertical distribution of the water content ratio of mud was investigated experimentally, and numerical simulations on the change in the water content ratio in the mud layer were made. Then, a simple one-dimensional numerical model was developed to predict the muddy bottom deformation under waves as well as the wave height decay. Wave flume experiments were carried out and the measured changes in the bottom topography and wave height were compared with the calculations.

2 Vertical distribution of water content ratio in mud layer

2.1 Experiments

The water content ratio of soft mud strongly affects its rheological properties and the vertical distribution of the water content ratio is significant for estimating mud motion. In order to clarify the effects of wave action on the change in the water content ratio in mud layers, two groups of experiments have been performed using commercial kaolinite; one for static water loading and the other for regular wave loading.

In the first group of experiments, a plastic square tank with a side length of 45cm and a plastic circular bucket with a radius of 38cm were used. The depths of the newly mixed mud in the tank and the bucket were set to about 14.4cm and 12.1cm, respectively, above which water was poured to 30cm and 26cm depth in order to allow comparison with the other group of experiments.

During the experiments the vertical distribution of the water content ratio of the soft mud was measured for about 220 hours and the results from one test is shown in Fig. 1. Meanwhile, the settlement of the mud layers in the containers were also observed, and the results were displayed in Fig. 3.

Figure 1 indicates that the change in the water content ratio by mud consolidation is large near the fixed bed and small in the surface layer.

The other group of experiments on the effects of wave action were performed

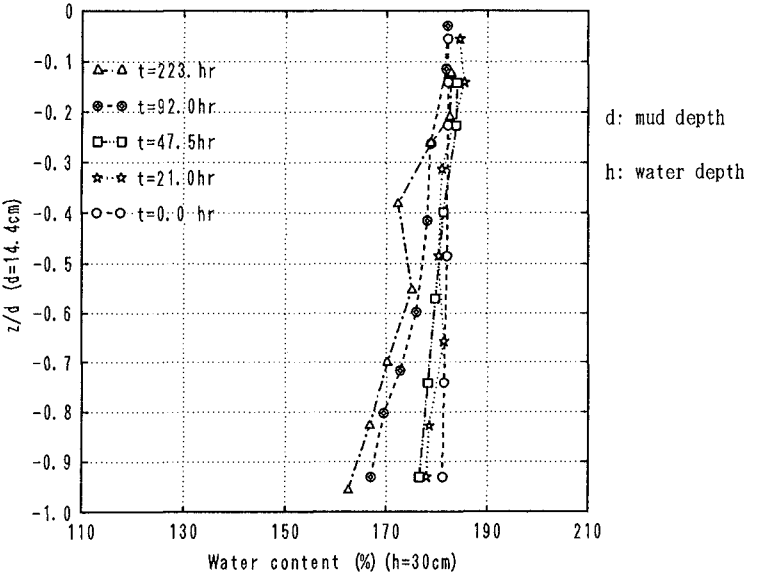

Figure 1: Change in water content ratio in still water

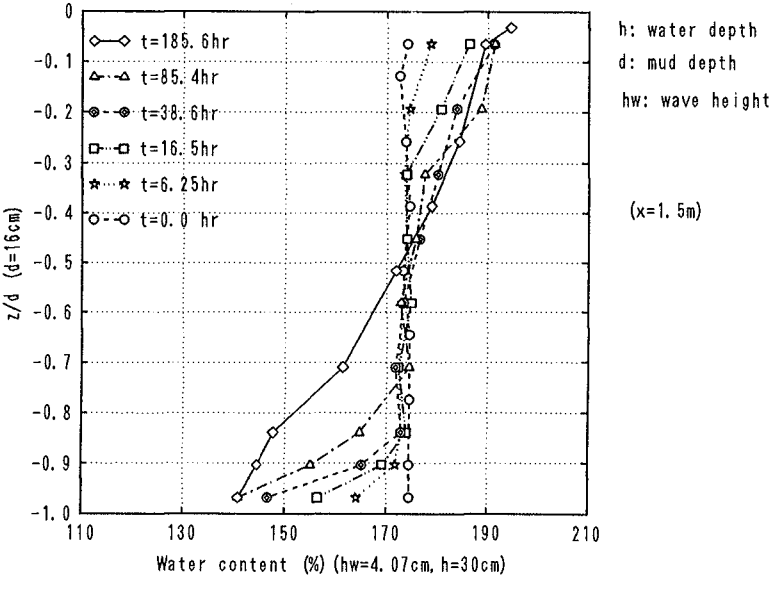

Figure 2: Change in water content ratio under waves (WE93A.15)

Table 1: Experimental conditions on change in water content ratio

Run	Mud depth (cm)	Period (s)	Water content (%)	Wave height (cm)
WE92E	16.4*(8,8.4)	1.02	(182, 120)	5.52
WE93A	16.0	1.02	175	5.20
WE93C	12.0	1.02	175	6.00

* two-layered bottom with a 8.0cm newly mixed upper layer and a 8.4cm consolidating lower layer

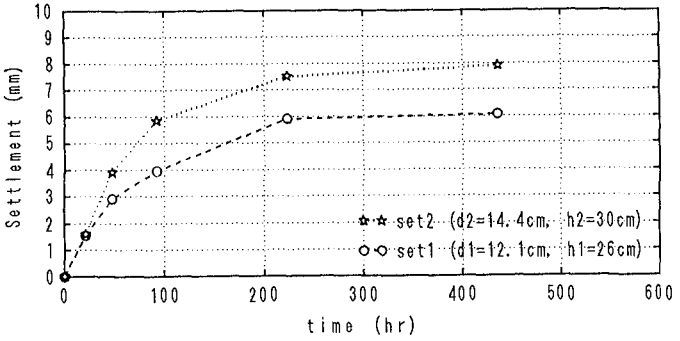

Figure 3: Settlement of mud layer in still water

in a large wave flume shown in Fig. 8, and the experimental conditions are summarized in Table 1. The water content ratio was measured at a few sections in the flume together with the distribution of the wave height and one typical example of the change in water content ratio is plotted in Fig. 2. This figure shows that the water content ratio in the surface layer increases with time due to the mud loosening whereas it decreases near the bottom because of the mud densification.

From the two groups of the experimental results, it can be seen that the change in the water content ratio of soft mud is caused by both wave action and self-weight. However, the roles of these two mechanisms are quite different. Gravity and static water only consolidate soft mud to consolidate whereas wave force can cause both "liquefaction" in the surface layer and densification in the lower layer of mud. Moreover, the densification produced by waves is much faster than that by static water and gravity. In addition, the position of the demarcation point of liquefaction and consolidation at a fixed section changes with the state of the mud consolidation.

The change in the water content ratio depends on both wave and mud layer properties. The influence of wave height on the change in the water content ratio has also been investigated experimentally, and the results are shown in

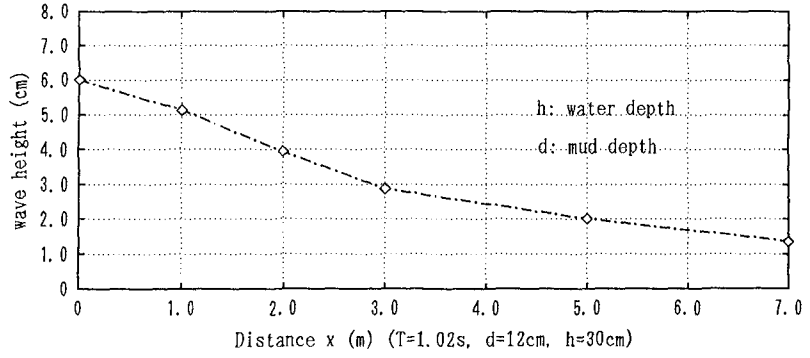

(a) Distribution of wave height measured in the x-direction(WE93C)

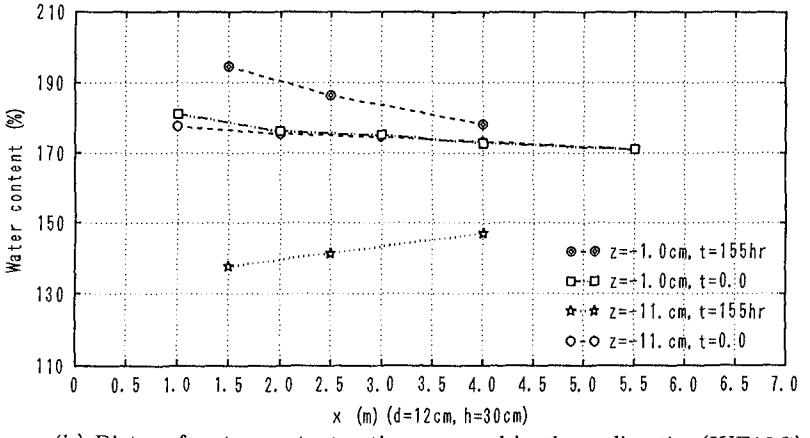

(b) Distr. of water content ratio measured in the x-direction(WE93C)

Figure 4: Influence of wave height on the change in water content ratio

Fig. 4. Figure 4b plots the distribution of the water content ratio measured in the on-offshore direction, and Fig. 4a depicts the corresponding wave height at the beginning of the experiment. The figure implies that a larger wave height produces a larger change in water content ratio.

2.2 Simulation of the change in water content ratio

The above experimental results suggest that wave action affects soft mud both through densification in the lower layer and liquefaction in the surface layer. Enlightened by the experimental investigation we first consider the two processes of mud consolidation and liquefaction separately, and then combine their effects on the change in the water content ratio linearly. We assume that mud densification which results in the decrease of the water content ratio is induced only by

the mud self-weight and the positive dynamic pressure or compressive stress, and reversely, that mud liquefaction which leads to the increase of the water content ratio is produced only by the negative dynamic pressure or tensile stress. Thus, the process of liquefaction is treated as the complete reversal of consolidation.

To describe the densification of the mud layer, the one-dimensional consolidation equation in soil dynamics is applied, and for general case written by,

$$\frac{\partial e}{\partial t} - \frac{\partial e}{\partial z}\left[g(e)\frac{\partial e}{\partial z}\right] - f(e)\frac{\partial e}{\partial z} = 0 \tag{1}$$

where the parameters $g(e)$ and $f(e)$ depend upon the wave properties as well as the mud characteristics. As a first step, those parameters are estimated using the following formulas which are based on limited experimental results, trial computations, and dimensional analysis,

$$g_c = \frac{k_c(e)}{\rho(1+e)}\frac{dp_m}{de}\left\{1 + \alpha_c\left(\frac{H_w}{L}\right)^{m_1}\left(\frac{H_w}{\sqrt{h\,d}}\right)^{m_2}\frac{k_c(e) - k_l(e)}{k_c(e) + k_l(e)}\right\} \tag{2}$$

$$f_c = \frac{\rho_m - \rho}{\rho}\frac{d}{de}\left\{\frac{k_c(e)}{1+e}\left[1 + \frac{k_c(e) - k_l(e)}{k_c(e) + k_l(e)}\right]\right\} \tag{3}$$

In the above equations e denotes the void ratio, k_c and k_l indicate the permeability in the conditions of compressibility and dilatation of mud, ρ_m and ρ are the densities of the mud and the sea water, p_m is the amplitude of the pore pressure, d the mud depth, H_w the wave height, L the wavelength, and h the water depth. The variables α_c, m_1, and m_2 are constants.

Following Been and Sills (1981), the governing equation can be solved with the appropriate boundary and initial conditions.

Next, we consider the loosening of mud under waves which is tentatively called "liquefaction" in the present study. Because the process of liquefaction is regarded as the reversal of consolidation, all of the assumptions and equations mentioned above can be applied to calculate liquefaction. The parameters $g(e)$ and $f(e)$ are expressed as follows,

$$g_l = \frac{k_l(e)}{\rho(1+e)}\frac{dp_m}{de}\left[\alpha_l\left(\frac{H_w}{L}\right)^{m_3}\left(\frac{H_w}{\sqrt{h\,d}}\right)^{m_4}\frac{k_c(e) - k_l(e)}{k_c(e) + k_l(e)}\right] \tag{4}$$

$$f_l = \frac{\rho_m - \rho}{\rho}\frac{d}{de}\left[\frac{k_c(e)}{1+e}\cdot\frac{k_c(e) - k_l(e)}{k_c(e) + k_l(e)}\right] \tag{5}$$

where α_l, m_3 and m_4 are constants.

Finally, the vertical distribution of the water content ratio under waves and gravity can be estimated by combining linearly the effect of consolidation and liquefaction. The depth of the liquefied mud layer is also determined through this combination.

As an example, Fig. 5 compares the calculated and measured vertical distribution of the water content ratio of mud under waves, and the values of the main

Table 2: Computational parameter values for the experiment

$k_c(e)/[\rho_f(1+e)]$	$k_l(e)/[\rho_f(1+e)]$	g_c	g_l	dp_m/de
4.0×10^{-11}	3.0×10^{-11}	7.2×10^{-9}	1.9×10^{-9}	18.0

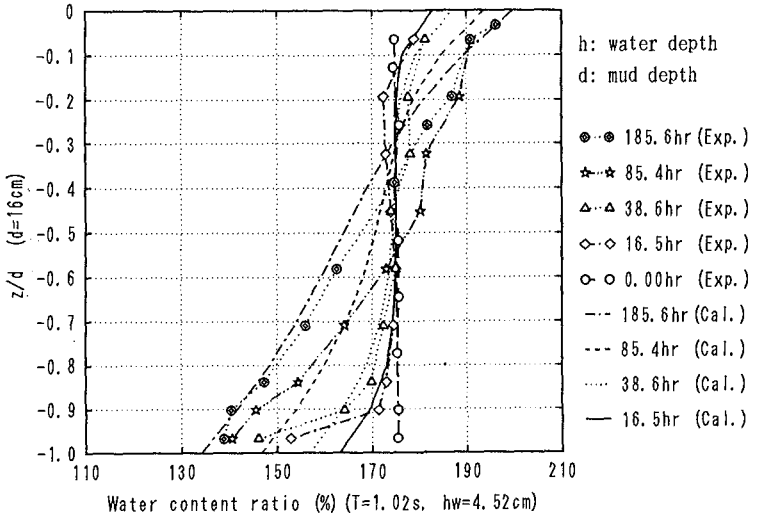

Figure 5: Comparison of the calculated and measured distribution of the water content ratio(WE93A.10)

parameters used in the computation are listed in Table 2. These values were determined by numerical experimentation. As can be seen from the figure, the calculated and measured shape of the vertical distribution agree well, but the magnitudes in the surface layer and near the fixed bed differ. This difference may partially be due to the neglect the nonlinear terms in the consolidation equations, and partially because of other model simplifications.

In summary, the simple model is applicable for predicting the vertical distribution of the water content ratio in the mud layer under wave action, keeping in mind the range of values employed in the experiment.

3 Muddy bottom deformation due to waves

3.1 Development of a topographical change model

Following the general structure of numerical models of sandy topography evolution, a one-dimensional numerical model of muddy bottom deformation is developed with a model structure as shown in Fig. 6. This model consists of three submodels for calculating 1) the vertical distribution of the water content ratio in the mud layer, 2) the wave deformation and mud motion, and 3) the mud transport rate and bathymetric change.

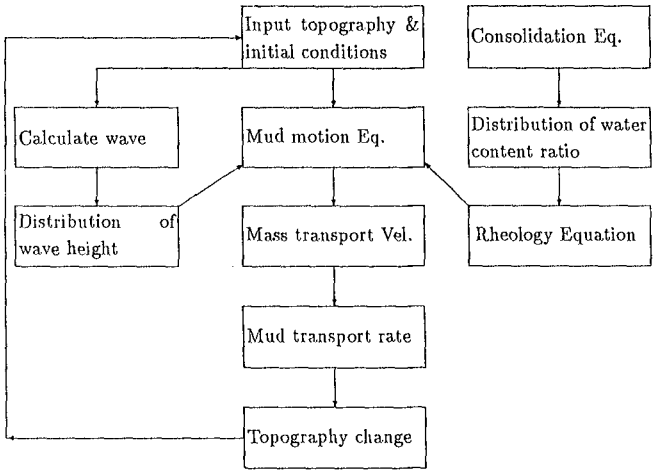

Figure 6: Structure of the numerical model of bottom change

First, let us discuss the calculation of the wave field. The mild-slope equation with the energy dissipation term is adopted to calculate the wave field,

$$\nabla \cdot (cc_g \nabla \phi) + (\sigma^2 \frac{c_g}{c} + i\sigma f_D)\phi = 0 \tag{6}$$

where $\phi(x, y)$ is the velocity potential on the mean free surface assumed to be

$$\Phi(x, y, z, t) = \phi(x, y) \frac{\cosh k(z + h)}{\cosh kh} e^{-i\sigma t} \tag{7}$$

and c and c_g denote the wave velocity and the group velocity, respectively, σ is the angular frequency, and k the wave number. The energy dissipation coefficient f_D varies both with the spatial coordinate and time and is defined as

$$f_D = \frac{\epsilon_D}{E} \tag{8}$$

where E is the wave energy intensity, and ϵ_D denotes the rate of energy dissipation per unit area estimated from the mud motion as,

$$\epsilon_D = \overline{\int_0^d \tau \frac{\partial u}{\partial z} dz} \tag{9}$$

where τ is the shear stress in the mud layer and u the local velocity. The symbol $\overline{\ }$ denotes the average over one wave period and d the fluidized mud depth.

For the two-dimensional case with a constant water depth the equation (6) becomes

$$\frac{d^2\phi}{dx^2} + \overline{k}^2 \phi = 0 \tag{10}$$

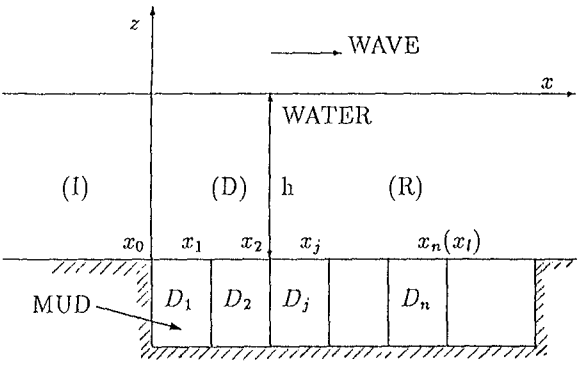

Figure 7: Definition sketch and coordinate system (Dissipation Area $0 < x < x_l$)

where

$$\overline{k}^2 = k^2 \left(1 + \frac{icf_D}{c_g \sigma}\right) \tag{11}$$

One case of wave propagation over a muddy bed in a wave flume is discussed here. As shown in Fig. 7, the wave field is divided into three regions. The damping region occupies (D) $0 < x < x_l$ and the flow domain extends to infinity ($x \to \pm\infty$). Wave breaking is assumed not to appear in the regions studied. In regions (I) and (R), there are no energy dissipation, $f_D = 0$, and the solutions to Eq. (10) is

$$\phi_I = -\frac{igH_w}{2\sigma}(e^{ikx} + K_R e^{-ikx}) \qquad x < 0 \tag{12}$$

$$\phi_R = -\frac{igH_w}{2\sigma} K_T e^{ikx} \qquad x > x_l \tag{13}$$

where $|K_R|$ and $|K_T|$ represent the reflection and transmission coefficients, respectively. The damping region (D) is furthermore divided into n subregions because the dissipation coefficient varies with both the spatial coordinate and time, and the velocity potential in the $j-$th subregion is

$$\phi_{D_j} = -\frac{igH_w}{2\sigma}(B_j e^{i\overline{k}_j x_j} + F_j e^{-i\overline{k}_j x_j}) \qquad x_{j-1} < x < x_j \tag{14}$$

where B_j and F_j are unknown constants to be determined and $j = 1, 2, ..., n$.

By using the continuity conditions for ϕ and its normal derivative, the unknown variables can be determined numerically from the following system of equations,

$$\phi_{D_j} = \phi_{D_{j+1}} \qquad \text{at} \quad x = x_j \tag{15}$$

$$\frac{d\phi_{D_j}}{dx} = \frac{d\phi_{D_{j+1}}}{dx} \qquad \text{at} \quad x = x_j \tag{16}$$

where $j = 0, 1, 2, ..., n$

For the simplest case $n = 1$, Liu *et al.* (1986) obtained an analytical solution for the equations given by

$$F = \frac{2\left(\frac{\bar{k}}{k} - 1\right)}{\left(\frac{\bar{k}}{k} + 1\right)^2 \exp(-2i\bar{k}x_l) - \left(\frac{\bar{k}}{k} - 1\right)^2} \tag{17}$$

$$B = \frac{2 - F\left(1 - \frac{\bar{k}}{k}\right)}{1 + \frac{\bar{k}}{k}} \tag{18}$$

$$K_R = \frac{2\left(1 + \frac{F\bar{k}}{k}\right) - \left(1 + \frac{\bar{k}}{k}\right)}{1 + \frac{\bar{k}}{k}} \tag{19}$$

$$K_T = \frac{2 - F\left(1 - \frac{\bar{k}}{k}\right)}{1 + \frac{\bar{k}}{k}} \exp\{i(\bar{k} - k)x_l\} + F\exp\{-i(\bar{k} + k)x_l\} \tag{20}$$

Next, we turn to the simulation of the mud motion. The interaction between the waves and a muddy bottom is very complicated mainly because of the complex characteristics of mud, especially its rheological properties. We have derived an empirical rheological equation based on another set of experiments (Shen *et al.*, 1993a), and it reads

$$\tau = G\epsilon - \tau_G \tanh(\alpha_G \epsilon) + \mu\gamma + \tau_0 \tanh(\alpha_\mu \gamma) \tag{21}$$

where τ is the shear stress, ε the shear strain, γ the shear rate, and G, τ_G, α_G, μ, τ_0 and α_μ are constants, of which G and μ represent the elasticity and viscosity, respectively. Most of the constant parameters can be determined by rheological experiments and expressed as functions of the water content ratio.

It has been recognized that the interaction between the waves and the muddy bed will result in bottom deformation which produces a mild slope at the mud surface. The local mild slope strongly affects the mud motion in turn. Including the effect of the mild surface slope, the one-dimensional linearized equation of mud motion is modified as

$$\rho_m \frac{\partial u}{\partial t} = -\frac{\partial p}{\partial x} + \frac{\partial \tau}{\partial z} - (\rho_s - \rho)g \sin\theta \tag{22}$$

where ρ_m, ρ_s and ρ denote the densities of the mud at any elevation, the mud at the surface layer and the water, respectively, θ represents the surface slope angle of the mud layer, u is the velocity of mud particles, p the dynamic pressure which is calculated from the solution of the mild-slope equation, and τ the shear stress evaluated by the proposed rheological relationship (21).

Numerical calculations have been carried out to solve the empirical rheological equation of soft mud, the mild-slope equation with the wave energy dissipation term, and the modified equation of mud motion.

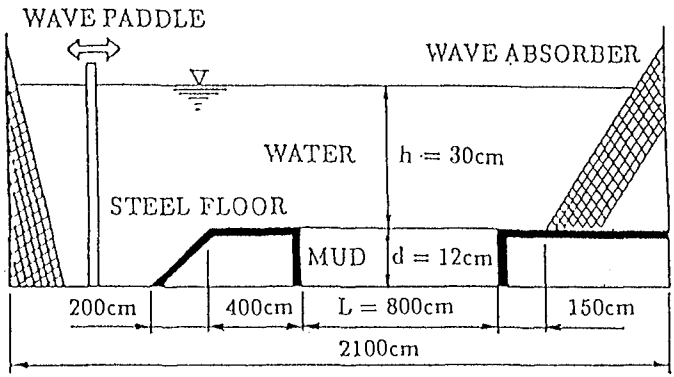

Figure 8: Experimental set-up

After obtaining the wave height change and the local velocity of the mud particles, the mass transport velocity can readily be estimated from the following formula used by Huynh *et al.* (1991)

$$U_L = U_E + \overline{\frac{\partial u}{\partial x}\int u\,dt} + \overline{\frac{\partial u}{\partial z}\int w\,dt} = U_E + U_S \tag{23}$$

where U_E represents the Eulerian average velocity and U_S the Stokes drift. For the one-dimensional case, they are evaluated by

$$U_S = \overline{(-\frac{1}{c}\frac{\partial u}{\partial t} - u\frac{f_D}{2c_g})\int u\,dt} \tag{24}$$

$$\mu'\frac{\partial^2 U_E}{\partial z^2} = -\frac{f_D}{c_g}\overline{\rho_m u^2}. \tag{25}$$

where μ' denotes the equivalent viscosity of mud.

Furthermore, the change in the local bottom elevation is computed by solving the conservation equation for sediment modified by Watanabe *et al.* (1984),

$$\frac{\partial z_b}{\partial t} = -\frac{\partial}{\partial x}(q_x - \epsilon_m|q_x|\frac{\partial z_b}{\partial x}) \tag{26}$$

where z_b denotes the change in the local elevation of the mud surface, ϵ_m is a positive constant which is determined empirically, and q_x is the sediment transport rate per unit width estimated by

$$q_x(x) = \int_0^d U_L dz \tag{27}$$

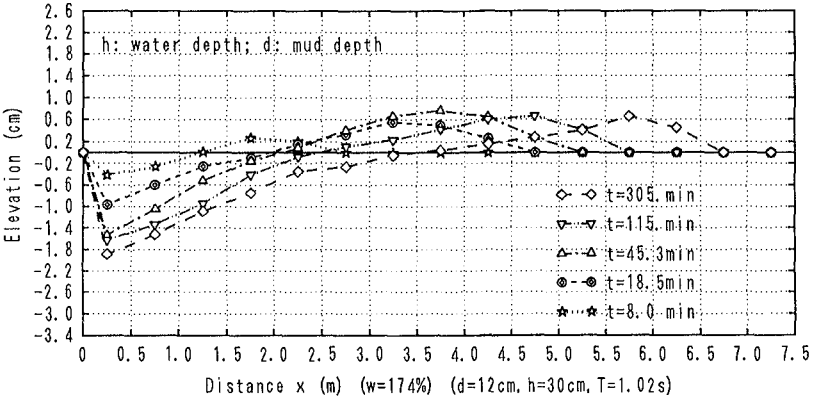

Figure 9: Change in the local elevation of the mud layer

3.2 Experiments and comparisons with calculations

Laboratory experiments were performed in a wave flume 21m long and 0.8m wide (Fig. 8) to verify the developed one-dimensional numerical model. The completely mixed commercial kaolinite (water content ratio: 174%) was placed in the middle of the flume. The depths of the mud and water layer were set to 12cm and 30cm, respectively. During the experiment for a few hours, measurements were made on the distribution of the wave height along the direction of wave propagation, the water content ratio of the mud layer, the concentration of the suspended mud, and the change in the local bottom elevations.

The measurements of the change in the local bottom elevation were not easily performed because (i) the suspension of the mud layer makes the water layer translucent or opaque and (ii) the mud layer is too soft to resist loading. Therefore, some instruments which works very well in sand are invalid for mud. Based on trial and error, a set of height gauge reequipped and a set of elevation meter newly made were used simultaneously to measure the change in the local elevation of the mud bottom and to correct the measured values.

As an example, Fig. 9 shows the experimental results in terms of the measured elevation change. From these results, some understanding of and conclusions on the topography change can be obtained as summarized in the following:

a) The eroded volume is a little larger than the deposited volume for a short time interval, and the difference increases with the loading time due to both the mud suspension and the settlement of the mud layer.

b) The peak of the deposited area moves slowly with the loading time in the direction of wave propagation. An erosion trough was always produced in the offshore direction. In addition, the mud surface slopes have a tendency to become smaller and smaller with the loading time.

c) The wave has a larger damping ratio for the newly mixed soft mud, and the

Table 3: Computational conditions and main parameter values

Run	Mud depth (cm)	Period (s)	Water content (%)	Wave height (cm)
WE93B	12.0	1.02	175.4	4.95
ρ_m (kg/m^3)	ρ_s (kg/m^3)	τ_0 (N/m^2)	μ (Ns/m^2)	G (N/m^2)
1300	1270	7.0	4.8	55

damping ratio will decrease with the loading time due to mud consolidation. It seems reasonable to conclude that only a fluidized mud layer plays a role in the wave dissipation. If the mud is completely consolidated, it may not absorb wave energy. In fact, this conclusion has also been arrived at through other experiments not discussed here.

Next, we attempt to apply the one-dimensional model for a simple case of mud motion in the flume. Some additional simplifications and assumptions are added here on the basis of the experimental results. Because the change in the water content ratio of the mud layer is very small for a relatively short time interval, as a first step, we neglect this change. Moreover, we suppose that mud consolidation for a relatively short time interval has so little effect on the rheology relationships that the influence can be ignored. The settlement of the mud layer and the transport of suspended mud are also omitted. In addition, the vertical two-dimensional mud motion near the starting point of the flume ($x = 0$) is simplified as one-dimensional by a so-called equivalent transforming of the local velocity of mud particles (Shen, 1993b).

Figure 10 compares the calculated and measured bottom change in the flume. The computational conditions and the main parameter values are listed in Table 3. It is seen that the calculated results of the bottom change have a similar tendency to the measured. However, at the right-hand side of the flume (downstream), the experimental results show that the mud motion stops at a certain position whereas the calculations can not simulate this phenomenon.

This discrepancy can be explained as follows. In the present one-dimensional model, an empirical rheology equation is utilized that implies mud will move under waves no matter how small the wave height is. In fact, the cohesive mud has a yield value that must be exceeded before the mud has a possibility to start moving. In addition, the simplifications and assumptions introduced in the present model have an effect on the prediction accuracy.

Figure 11 shows a comparison of the measured and calculated wave height distribution at the initial stage of an experiment, indicating a good agreement between them.

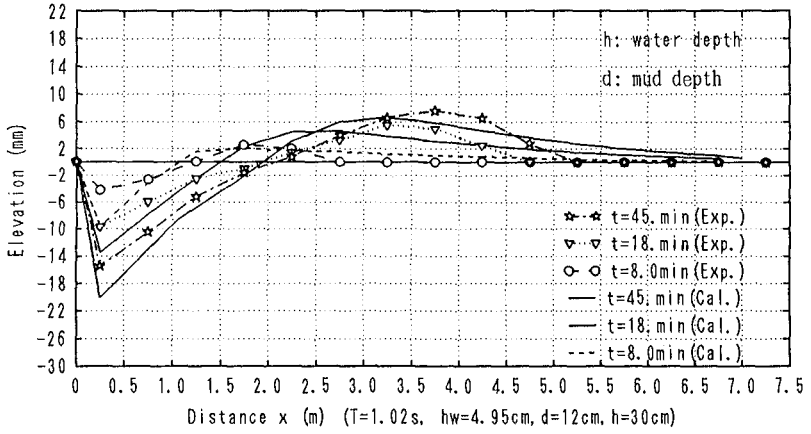

Figure 10: Comparison of measured and calculated bottom topography change in the flume

4 Conclusions

The present study focuses on investigating the vertical distributions of the water content ratio in a mud layer and numerical simulation of muddy bottom deformation and wave height decay.

The results of the first two groups of experiments have revealed that the change of the water content ratio is caused by both the wave action and the gravity of mud. However, the effects of wave action and gravity are quite different. The gravity only causes soft mud to consolidate, whereas the wave action can induce both the loosening in the surface layer and the consolidation in the lower layer of the mud. Numerical estimation of the change of the water content ratio in the muddy bed by the proposed simulation model has shown a similar tendency in the in the calculations as for the measurements.

A simple one-dimensional numerical model has been developed to predict the muddy bottom deformation under waves as well as the wave height decay. In conclusion, the one-dimensional model has been verified by the flume experiments to be applicable to predict the experimental phenomena, although its applicability is dependent on the accuracy of the rheological equation of mud.

Acknowledgement

The authors would like to express their appreciation to Prof. I. Towhata of Tokyo Univ., Japan, T. Shibayama of National Yokohama Univ., Japan, and M. Larson of Univ. of Lund, Sweden, for their helpful discussion. The present study was financially supported by the Grant-in-Aid for Scientific Research, Japanese

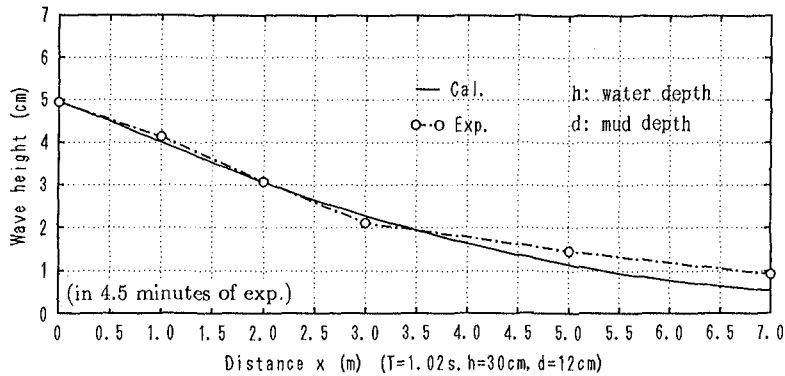

Figure 11: Comparison of measured and calculated wave height distribution

Ministry of Education, Science and Culture.

References

[1] Been, K. & Sills, G.C.(1981): Self-weight consolidation of soft soils: an experimental and theoretical study, *Géotechnique* 31, No. 4, pp. 519-535.

[2] Darymple, R.A. and Liu, P.L.-F.(1978): Waves over soft muds: a two-layer fluid model, J. Physical Oceanogr., Vol. 8, pp. 1121-1131.

[3] Gade, H.G (1958): Effect of nonrigid, impermeable bottom on plane surface waves in shallow water, J. Marine Res., Vol. 16, No. 2, pp. 61-82.

[4] Huynh, T.N., M. Isobe and A. Watanabe(1991): Study on the mud mass transport under waves on basis of the rheology properties of mud, Proc. Japanese Conf. on Coastal Eng., Vol. 38, pp. 466-470 (in Japanese).

[5] Mei, C.C. and K.F. Liu(1987): A Bingham-plastic model for a muddy seabed under long waves, J. Geophys. Res., Vol. 92, No. 13, pp. 14581-14594.

[6] Liu, L.-F., *et al.* (1986): Wave reflection fron energy dissipation region, J. Waterway, Port, Coastal and Ocean Eng., Vol. 112, No. 6, pp. 632-644.

[7] Shen, D.X., M. Isobe and A. Watanabe (1993a): Mud mass transport under waves based on an empirical rheology model, Proc. of 25th IAHR, Vol. 4, pp. 120-127.

[8] Shen, D.-X.(1993b): Study on mud mass transport and topography change of muddy bottom due to waves, Doctoral dissertation of Tokyo University, 165pp.

[9] Shibayama, T. and An, N.N.(1993): A visco-elastic-plastic model for wave-mud interaction, Coastal Eng. in Japan, vol. 36, No. 1, JSCE, pp. 67-89.

[10] Watanabe A., *et al.* (1984): Three-dimensional numerical model of beach deformation with the onshore structures, Proc. Japanese Conf. on Coastal Eng., Vol. 31, pp. 406-410 (in Japanese).

[11] Yamamoto, T., H.S.L. Koning and E. Van Hijum(1978): On the response of a pore-elastic bed to water waves, J. Fluid Mech., Vol. 87, Part 1, pp. 193-206.

[12] Zen, K. *et al.* (1990): Oscillatory pore pressure and liquefaction in seabed induced by ocean waves, J. of Soils and Foundations, JSCE, Vol. 30, No. 4, pp. 147-161.